Sustainable Energy & Fuels

Pilot-scale hydrotreating of catalytic fast pyrolysis biocrudes: Process performance and product analysis

Journal:	*Sustainable Energy & Fuels*
Manuscript ID	SE-ART-04-2021-000540.R1
Article Type:	Paper
Date Submitted by the Author:	26-Jul-2021
Complete List of Authors:	Verrdier, Sylvain; Haldor Topsoe AS Mante, Ofei; RTI International Hansen, Asger; Haldor Topsoe AS Poulsen, Kristoffer; University of Copenhagen Faculty of Science, Plant and Environmental Sciences Christensen, Jan; University of Copenhagen Faculty of Science, Plant and Environmental Sciences Ammtizboll, Nadia; Haldor Topsøe A/S Gabrielsen, Jostein; Haldor Topsoe AS Dayton, David; RTI International

ARTICLE

Pilot-scale hydrotreating of catalytic fast pyrolysis biocrudes: Process performance and product analysis†

Received 00th January 20xx,
Accepted 00th January 20xx

DOI: 10.1039/x0xx00000x

Sylvain Verdier[a], Ofei D. Mante[b], Asger B. Hansen[a], Kristoffer G. Poulsen[c], Jan H. Christensen[c], Nadia Ammtzboll[a], Jostein Gabrielsen[a], David C. Dayton*[b]

Catalytic fast pyrolysis (CFP) is a technology option for producing advanced biofuels from hydrocarbon-rich biocrude intermediates. The relatively high oxygen content of biocrudes compared to petroleum intermediates increases hydrogen consumption and the lower thermal stability accelerates catalyst deactivation and reactor fouling hindering the adaptation of hydrotreating technology for biocrude upgrading into biofuels. In this study, four chemically different biocrude feeds were upgraded in a pilot scale hydroprocessing unit at similar process conditions using a commercial hydrodeoxygenation (HDO) catalyst. The biocrude feeds and hydrotreated products were characterized using standard ASTM procedures and advanced analytical techniques (GC×GC-FID and GC×GC-MS). HDO catalyst activity was monitored by changes in physical properties and chemical composition of the upgraded products as a function of time on stream. Aliphatic acids, ketones, aldehydes, and furan derivatives were completely converted during the hydrotreating tests while the concentration of aromatics, aliphatic hydrocarbons and phenolics increased during the hydrotreating tests. The oxygen content, nitrogen content, specific gravity, viscosity and the heavy end of the boiling point (determined by simulated distillation) of the upgraded products increased with increasing time on stream during hydrotreating. The deactivation rate was the lowest for the biocrude feed that contained the most aliphatic and aromatic hydrocarbons and was the highest for the biocrude feed that had the most anhydrosugars. Overall, the HDO deactivation rate correlates with the total amount of oxygen in the feed (17 wt% to 29 wt%, on a wet basis).

Introduction

The International Energy Agency (IEA) predicts in the 2018 World Energy Outlook that the share of renewables in the pool of transport fuels will increase to 6% or 16% in 2040 depending on the scenario ("New Policies Scenario" and "450 Scenario" respectively).[1] The source of these renewable transport fuels will come from a variety of technologies for producing different biofuels such as: bioethanol (produced by fermentation of starch-based or molasses-based sugars), biodiesel[2] (aka. FAME produced by transesterification of oils, fats, and grease), renewable diesel[3] (produced by hydrotreating vegetable oils, animal fats, or used cooking oils), and renewable gasoline, diesel, and jet fuel produced by upgrading biomass liquefaction or pyrolysis intermediates (biocrudes)[4-10] or hydrotreating pulp and paper byproducts like tall oil.[11, 12] Currently, bioethanol and biodiesel represent most of the global renewable transport fuel production (74% and 22% respectively in 2017), while the amount of processed vegetable oils keeps increasing (4% in 2017).[13]

Catalytic and non-catalytic lignocellulosic biomass pyrolysis technologies are being thoroughly investigated to produce hydrocarbon-rich liquids (bio-oil or biocrude) that can be upgraded using conventional hydroprocessing technology. Note that other types of feedstocks such as algae,[4, 14] plastic wastes,[15-17] and scrap tires[18, 19] to name a few, can also be pyrolyzed to produce biocrudes.

Extensive references and reviews about pyrolysis can be consulted for more details about the technology and the influence of operating parameters and feedstock type[5, 20, 21] (and references therein) on biocrude yield and quality. Unlike slow and fast pyrolysis, catalytic fast pyrolysis (CFP) is being developed to produce low oxygen containing biocrudes.[5, 21-24] The purpose of using a catalyst during fast pyrolysis is to improve biocrude processability by increasing thermal stability, decreasing corrosiveness, improving miscibility with fossil fuels, and minimizing the levels of catalyst contaminants (typically P, Na, Ca and K), among other things.[22, 23]

Biocrude upgrading to finished biofuels and blendstocks by adapting catalysts and process conditions in conventional hydroprocessing technology has been extensively studied in recent years at laboratory and pilot scale. For example, details about the two possible routes to upgrade biocrude, hydrodeoxygenation (HDO) and zeolite cracking, are presented in the literature.[25] Furthermore, Gollokota et al.[26] evaluate

[a] Haldor Topsoe A/S, Haldor Topsøes Allé 1, 2800 Kgs. Lyngby, Denmark.
[b] RTI International, 3040 E. Cornwallis Road, Research Triangle Park, NC 27709, USA.
[c] Department of Plant and Environmental Sciences, Faculty of Science, University of Copenhagen, Thorvaldsensvej 40, 1871 Frederiksberg, Denmark

† Footnotes relating to the title and/or authors should appear here.
Electronic Supplementary Information (ESI) available: [details of any supplementary information available should be included here]. See DOI: 10.1039/x0xx00000x

various upgrading processes, such as catalytic cracking, HDO, steam processing, esterification, and the use of supercritical fluids. Regarding HDO, they list advantages of various types of catalysts, including conventional sulfided alumina-based catalysts. Elliott[27, 28] summarizes upgrading biocrudes produced from biomass hydrothermal liquefaction and various pyrolysis processes from several research groups. The influence of operating conditions such as space velocity, catalyst type and the potential for using hydrogen donor solvents are discussed. Al-Sabawi and Chen,[29] address many of the issues previously discussed in the aforementioned references but also describe co-processing bio-derived intermediates with petroleum feedstocks. Melero et al.[30] discuss the challenges of integrating biocrudes in existing refineries, such as hydrogen consumption, CO and CO_2 formation, and poorer cold flow properties. Furimsky[31] presents a complete overview of the processes to convert biomass into bio-derived intermediates, with an emphasis on upgrading algae oils and biocrudes from lignocellulosic biomass and sewage sludge pyrolysis. Talmadge et al.[32] provide a review on various strategies for refinery integration of pyrolysis oils, including how these feedstocks could be used in a fluid catalytic cracking (FCC) unit and a hydrotreater.

Understanding the chemical composition of biocrudes is beneficial for developing robust upgrading strategies; however, analysis of biocrudes is challenging because of their complex nature that includes highly functionalized components with very broad boiling ranges and molecular weight distribution (including oligomers) and high concentration of thermally labile and reactive oxygenates. Several groups, such as VTT (Technical Research Centre of Finland) in Finland, and the National Renewable Energy Laboratory (NREL) and the Pacific Northwest National Laboratory (PNNL) in the United States, have gone to great lengths to develop methods for measuring physical properties and chemical compositions of pyrolysis oils.[33-35] Round-robin studies of five major bio-oils were performed between 1988 and 2012 leading to the development of ASTM D7544, a standard method that details the specifications for pyrolysis liquid biofuel for use in industrial burners. This standard focuses on water content (measured by Karl Fischer titration), density, pH, Total Acid Number (TAN) measured by potassium hydroxide titration, and kinematic viscosity. Another recent round-robin study was also conducted by NREL to update and validate various techniques for biocrude analysis with reasonable measured accuracy.[34] Gas chromatography with mass spectrometric detection (GC-MS) was selected for identification of selected compounds. A modified TAN titration method was developed to differentiate between naphthenic acids and carboxylic acids (Carbonyl Acid Number and Total Acid Number – CAN/TAN). A ^{31}P NMR method[34] was also recommended for functional group identification.

Independently, standard chromatographic techniques cannot comprehensively identify all oxygenates because these components are reactive and thermally labile. The literature related to analysis of renewable feedstocks and the related challenges is quite extensive. Stas et al.[36, 37] summarized various techniques for sample preparation and listed some of the main contributions based on GC, GC×GC, high-resolution mass spectrometry, NMR, and FTIR. Michailof et al.[38] detail pyrolysis oil characterization with GC×GC, LC×LC, FT-ICR and 2D-NMR. Kanaujia et al.[39] review the sample preparation techniques and the standard methods applicable to measure the physical properties and chemical composition of pyrolysis oils including references about TGA, GC, mass spectrometry and NMR. Mohan et al.[20] provide a short but useful introduction about the characterization of wood-based pyrolysis oils, sample preparations, and characterization of oxygenates.

The goal of this study is to provide complimentary understanding of the impact of the biocrude physical properties and chemical composition on HDO catalyst performance during biocrude upgrading in a continuous flow pilot-scale hydrotreating reactor system.[40] Four different biocrude samples were produced from CFP of loblolly pine in a nominal 1 ton per day (1TPD) pilot scale unit.[22, 23, 40] Comprehensive analysis of these four CFP biocrude samples was conducted using standard ASTM methods and advanced analytical methods such as two-dimensional gas chromatography and mass spectrometry.[41] Pilot scale hydroprocessing [40, 42] of these four biocrude samples was conducted at essentially the same process conditions and upgraded products collected as a function of time on stream were analyzed using the same advanced analytic methods used to analyze the biocrude feeds. Hydrotreating catalyst performance was assessed as a function of changes in the physical properties and chemical compositions of the upgraded products. A summary of the hydrotreating experiments, including the measured physical properties and detailed chemical characterization of upgraded products as a function of time on stream, begin to reveal correlations between biocrude composition and HDO catalyst performance and deactivation rates under commercially relevant process conditions to guide future technology scale up and demonstration.

Experimental

Biocrude production

Biocrude samples were produced in a 1TPD catalytic biomass pyrolysis unit that includes a biomass feed system, continuously circulating fluidized bed reactor, and a product recovery section. This unit has been described in detail in the literature.[22, 23] The biocrude intermediates for this study were produced by metering loblolly pine sawdust into the pyrolysis mixing zone using a screw feeder where it contacts hot, regenerated non-zeolitic gamma alumina catalyst with a nominal (D_{50}) particle size of 72 µm (T-2610 alumina microspheres commercially available from Clariant). Nitrogen is introduced into the bottom of the mixing zone to maintain a well-fluidized bed and maximize contact time between biomass and hot catalyst during pyrolysis. Catalyst and biomass pyrolysis products are transported through the riser section of the reactor to the inlet of a cyclone to separate entrained solids (char and catalyst) from pyrolysis vapors and permanent gases. The separated solids are transferred to the bubbling fluidized bed regenerator

where catalyst coke and char are oxidized to regenerate the catalyst and provide heat to drive the endothermic biomass pyrolysis process. Pyrolysis temperature (400-600°C) is maintained by balancing the biomass federate and the temperature and circulation rate of the regenerated catalyst. Standard operating conditions establish a ~0.75 sec total residence time in the mixing zone at nominally ambient pressure.

The pyrolysis vapors are condensed by a direct contact spray quench. Water is atomized at the inlet of the quench system and mixed with the pyrolysis vapors to remove sensible heat. The quenched vapors and gases pass through a gas/liquid separator, a coalescing filter, a shell-in-tube heat exchanger, and a second coalescing filter, respectively. Most of the aqueous fraction (water and water-soluble organics) is collected in the gas/liquid separator while the pyrolysis aerosols and permanent gases pass through to the first coalescing filter operated at 90-110°C to collect the majority of the CFP biocrude product, designated as the heavy fraction. The remaining vapors and permanent gases then pass through a heat exchanger to cool the product gases to approximately 5-10°C. Light organics, designated as the light fraction, and any remaining aerosols and water vapor are collected in the second coalescing filter. Remaining permanent gases are sent through a pressure control valve to a thermal oxidizer. The aqueous and organic biocrude fractions are collected separately. Additional details about the design and operation of the 1TPD CFP unit are available in the literature.[22, 23, 40]

The operating conditions in the 1TPD catalytic biomass pyrolysis unit for producing the four biocrude samples relevant to this study are listed in Table 1. One light fraction (F1), one heavy fraction (F5) and two blends of light and heavy fractions (F3 and F4) were produced from biocrude products collected during the same CFP run. Note that the average pyrolysis temperature ranges between 465 and 575°C. Also, F5 was sampled at the end of the run and differs from that collected at the start of run. It might therefore not be representative of the operating conditions in the 1TPD unit. The sample designations in Table 1 are same used in Table 1 of reference 41[41] for consistency.

Table 1. Summary of operating conditions used for CFP loblolly pine biocrude production in RTI's 1TPD catalytic biomass pyrolysis unit described in references 22 and 23.

CFP biocrude product	Feed F1	Feed F3	Feed F4	Feed F5
Average pyrolysis temperature	520°C			575°C
Average apparent vapor residence time in mixing zone	1.41 s			0.75 s
Nominal Biomass Feedrate	38 kg/h[23]			51 kg/h
Production Duration	30 hours[23]			7 hours
Biocrude Yield	11.5 wt% carbon[23]			
Fraction from CFP unit	Light	15% Light + 85% Heavy		Whole

Hydrotreating studies

A pilot-scale dual reactor hydroprocessing unit was used for hydrotreating (HDT) biocrude to produce upgraded HDO products.[40] The pilot-scale unit includes two 44-L feed tanks and high-pressure liquid metering pumps for feeding biocrude samples separately or co-feeding biocrude with other hydrocarbon liquids. Two 350-mL fixed bed reactors with a 1.22-m reaction zone can be used separately or in series to test single catalysts over a wide ranges of space velocities or multiple combinations of different catalysts. The design temperature is 450°C with a maximum operating temperature of 430°C and the design pressure is 200 barg with a maximum operating pressure of 172 barg.

Upgraded product and gas (mostly hydrogen) are first separated in a high-pressure separator (HPS). The liquid product from the HPS is sent to a low-pressure stabilizer (LPS), then to a nitrogen stripper for removal of gases and other non-condensed light hydrocarbons (naphtha). The exit gases from the HPS and LPS were combined prior to sampling. Six automated sampling ports are available to collect the combined oil/water product for mass balance determination and five sequenced samples for collecting upgraded hydrocarbon products as a function of time on stream. The sequenced samples are intended to evaluate short-term catalyst performance based on upgraded product composition. Catalyst dilution and concentration along the length of the reactor are used to maintain appropriate catalyst activity and manage the exothermic heat of reaction. Process conditions are carefully controlled, specifically temperature is controlled and varied in six zones along the length of the reactor. Careful preparation is necessary to evaluate catalyst performance and to determine if catalyst deactivation rates meet or exceed targets defined for successful commercial-scale application. The catalyst was diluted with an inert material (60 mesh SiC) using a 60 vol% SiC/40 vol% catalyst ratio. Additional details about the design and operation of the hydroprocessing unit are available in the literature.[40]

Table 2. Operating conditions used during hydrotreating (HDT) pilot plant tests.

HDT experiment	Exp. A	Exp. B	Exp. C	Exp. D
Biocrude Feed	Feed F4	Feed F3	Feed F1	Feed F5
Total Time on stream (hours)	103	365	118	62
Reason test ended	Shut-down	Shut-down	Lack of feed	Plug
H_2 partial pressure (barg)	138	138	138	138
Average Temperature (°C)	300	290	300	290
LHSV (h^{-1})	0.25	0.25	0.25	0.35
H_2/oil ratio (Nl/l)	3000	3300	3300	3300

The selected biocrudes were produced from the same biomass (loblolly pine) and the same catalyst in the 1TPD CFP unit, but they provide a range of total oxygen content and variable chemical composition because of the varying operating conditions. As shown in Table 2, Exp. A and B were conducted with biocrudes F3 and F4 that were produced in the CFP unit during the same run. Note that biocrude F2 presented in the previous study[41] is not discussed here because it was the only sample hydrotreated in two-stages (first step at low temperature and second step at standard hydrotreating

conditions) and comparison to the single-stage hydrotreating experiments with the other biocrudes was not applicable.

The NiMo-based hydroprocessing catalyst (TK-341) used for the biocrude upgrading study is a commercial catalyst manufactured by Haldor Topsoe A/S that has high HDO activity and moderate hydrodesulfurization and hydrodenitrification activities. The catalyst was sulfided prior to each experiment with a 10% H_2S in hydrogen blend using a prescribed protocol. The operating conditions for the hydrotreating experiments are also listed in Table 2 as is the total time on stream for each of the four experiments. Some experiments were stopped because of scheduled shut-down (Exp. A and B) or lack of feed (Exp. C) while one experiment was stopped because of excessive pressure drop caused by reactor plugging (Exp. D conducted with the heavy fraction, Feed F5).

Standard analyses

Standard analyses of the biocrudes and the hydrotreated products were conducted according to the ASTM standards listed in Table 3. Analyses were performed in Haldor Topsoe's analytical laboratory except for moisture content, that was measured at RTI following the ASTM E203 standard test method for water using Hydranal-composite 5 K reagent in Karl-Fischer titration, and oxygen that was measured by DB Lab A/S (Denmark) using a Perkin Elmer 2400 Series II analyzer.

Table 3. Summary of standard analytical methods

Analyses	Standard Method
S	ASTM D4294
N	ASTM D5762 or D4629
H	ASTM D7171
C	ASTM D5291
O	Perkin Elmer 2400 Series II analyzer
Moisture	ASTM E203
Ca, Fe, K, Mg, Na, P, Si	In-house developed methods using ICP-MS and ICP-OES inspired by ASTM D5708
Simulated Distillation	ASTM D7213C

Sample preparation

The samples were analyzed either as received (i.e. non-fractionated) or were fractionated for further analysis following the method discussed by Kristensen et al.[41] The fractionation method was adapted from Oasmaa et al.[43, 44] that separates biocrudes and upgraded products into water soluble (WS) and water insoluble (WIS) components. Sample preparation required acetone, tetrahydrofuran (THF) (analytical grade, ≥ 99.0%) and tetrachloromethane (CCl_4) (analytical grade ≥ 99.5%) purchased from Sigma-Aldrich. The non-fractionated biocrudes and WIS fractions were dissolved in THF (1:1, v/v). A quality control (QC) sample was prepared by dissolving a dewatered non-fractionated crude pyrolysis oil in THF in a 1:1 v/v ratio. A light gas oil dissolved in tetrachloromethane (CCl_4) in a 4:1 v/v ratio was prepared as a reference standard. The mass balances reported for fractionating biocrudes F3, F4, and F5 in Kristensen et al.[41] were 88.6%, 91.0%, and 101.9%, respectively. The mass balance for biocrude F1 fractionation was only 46.9% because light components were lost during sample drying.

Sample chemical analysis

Two-dimensional gas chromatography with flame ionization detection (GC×GC-FID)

In this study, all four biocrudes and 16 hydrotreated products were analyzed using a Thermo GC×GC-FID instrument with an AI 3000 autoinjector, a programmed temperature vaporizing (PTV) inlet, a dual-jet two-stage cryogenic (liquid CO_2) modulator and a flame ionization detector (FID). The Thermo Chrom-Card and the HyperChrom® GC×GC software (ver. 2.4.1) were applied for instrument control, data acquisition and analysis. The column system contained two serially connected fused silica columns including a Rtx-1701 (30m, 0.25mm id., 0.25 µm film thickness) as 1D column and a Rxi-5Sil MS (1.5 m, 0.15 mm id., 0.15 µm film thickness) as 2D column. The GC oven was programmed from 40° to 300°C at 2.5°C/min and the He carrier gas flowrate was 1.5 mL/min. The water insoluble (WIS) biocrude fractions and non-fractionated biocrudes were analyzed with an 8 sec modulation period that was increased to 9 sec for the WIS fractions of the upgraded product samples. The WIS fractions of both biocrudes and upgraded products were analyzed with the PTV injector operating in solvent-vent mode at 60° C for 1 min to evaporate the THF solvent and then rapidly heated to 350°C for 1 min during sample transfer. The PTV was operated in split mode with a split ratio of 1:100 and rapidly heated to 350° C for 2 min for sample transfer when analysing the non-fractionated biocrudes. The sample size of all samples analysed was 0.3 µL.

Duplicate non-fractionated biocrude feed samples were analysed in two batches together with THF solvent blanks, WIS fraction blanks, the QC sample, and the reference standard. Note that only the analyses of the water-insoluble THF fractions (WIS) of the non-fractionated biocrudes and hydrotreated samples are reported in this study for comparison. The WIS fraction accounts for ~80 vol% of the biocrude samples[41] and an even higher percentage of the hydrotreated products, depending on the oxygen content.

Two-dimensional gas chromatography with mass spectrometric detection (GC×GC-MS)

The same samples described above and in similar batches were also analyzed by GC×GC-MS using a LECO Pegasus 4D instrument comprising a 7693A ALS, a Gerstel CIS-4 inlet, a quad-jet two-stage cryogenic (liquid N_2) modulator, a secondary oven and a time-of-flight mass spectrometer (TOF-MS). LECO ChromaTof® GC×GC software (ver. 4.70) was used for instrument control, data acquisition and analysis. The same column system, GC oven temperature, and PTV injector mode used in the GC×GC-FID method described above were used for GCxGC-MS analysis. The secondary oven was operated with a 5°C offset to the main oven and the modulator with a 15° C offset to the secondary oven. The MS was operated at an acquisition rate of 100 Hz in a m/z range of 41 to 541, and with a source temperature of 225°C.

Data analysis

The results from the GCxGC-MS and GCxGC-FID analyses were combined to identify specific compounds that were grouped into specific compound classes for semiquantitative comparison

between samples. For each peak with a signal-to-noise ratio greater than 10 (S/N > 6 for subpeaks) identified in the GCxGC-MS 2D color plots, a list of the ten most probable compounds with a search match greater than 600 were found by comparing peaks' caliper and true peak spectra with searches in the NIST MS library (NIST 08). Compound classes were composed based on the tentatively identified compounds in the GCxGC-MS data set. Identical samples were analyzed by GCxGC-FID using exactly the same analytical protocol to achieve the same 1D and 2D chromatographic separations. Therefore, integration windows in the GCxGC-FID color plots could be established for the compound classes identified by GCxGC-MS. The area for each compound class was integrated using proprietary software developed at the University of Copenhagen that includes preprocessing for baseline subtraction and peak alignment. Area counts for identified compound classes can be normalized in two ways: 1) by normalizing to the sum of area counts for all compound classes giving the Area-%, and 2) by normalizing to the area counts for selected compound classes to the area counts for the aliphatics compound class. The results presented in this study are the Area-% for all compounds classes while the results in our previous study were normalized to the aliphatics compound class.[41] Ultimately, averages of three replicate samples were calculated. The standard deviations (less than 5%) and relative standard deviations (less than 50%) of the compound classes identified in the whole and fractionated biocrude compositions were discussed in detail in the literature.[41]

When comparing the true peak mass spectrum of a specific compound with that of NIST reference spectrum, the most probable hit with a search match greater than 600 was not always chosen. The position of the peak in the 2D chromatogram and the base peak in the mass spectrum together with the NIST reference match were all considered for tentatively identifying a compound. The peaks with a search match less than 600 were not tentatively identified and assigned a structure. However, the mass spectra associated with several of these peaks indicated that oxygen was part of the molecule. If the position of the unassigned peak in the 2D chromatogram was closely associated with firmly assigned O-containing compounds it was considered an "unknown oxygenate."

Carbon-13 nuclear magnetic resonance (^{13}C-NMR)

^{13}C-NMR spectroscopy was performed on the non-fractionated biocrude samples using a JOEL 300 MHz NMR spectrometer (JEOL Ltd, Tokyo, Japan). About 1.0 g of biocrude was dissolved in 0.7 ml of dimethyl sulfoxide-d6 in a 5 mm sample tube. The NMR solvent, DMSO-d6 (99.9 atom % D, containing 1% [v/v] tetramethylsilane [TMS]) was obtained from Sigma-Aldrich (Sigma-Aldrich, St. Louis, MO, USA). The observing frequency for the ^{13}C nucleus was 100.58MHz. The pulse width was 5.8 µs, the acquisition time was 1.37 s, and the relaxation delay was 2 s. The spectra were obtained with 8000 scans and a sweep width of 23.8 KHz.

Results and Discussion

Biocrude Analyses

Table 4 shows the elemental composition (wt%), moisture content (wt%), inorganic impurities content (wt ppm), and simulated distillation results for the four (non-fractionated) biocrudes. Note that simulated distillation was not performed on the most oxygenated, least thermally stable biocrude F5. The SimDist curves are consistent with the typical fractions from the CFP unit, i.e. the light fraction has components with the lowest boiling points. Moisture content varies between 8 and 10.4 wt%. The oxygen contents ranged from 17 wt% to 29 wt%, on a wet basis. With respect to the inorganic impurities (Ca, Fe, K, Mg, Na, P, and Si), the most oxygenated biocrude F5 had the highest concentration of metals. However, the relative distribution amongst these inorganic contaminants is relatively constant as seen in Figure 1.

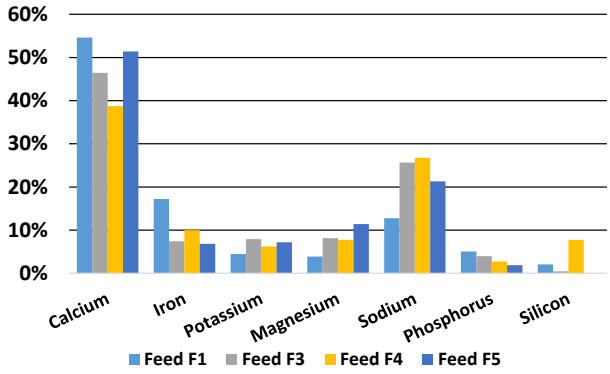

Figure 1: Normalized distribution of contaminants in the four CFP biocrude feeds

Sixteen compound classes were identified by GC×GC-MS, including unknowns, and integrated for each sample. The 16 compound classes were pooled into six groups that seem to best represent the composition of the lignocellulosic feedstock (loblolly pine) and fast pyrolysis thermal decomposition reactions; namely: Group A: aliphatics (paraffins and naphthenes); Group B: aromatic compounds (abietic acid derivatives and mono-, di- and triaromatics); Group C: smaller aliphatic acids and aldehydes/ketones (originating from cellulose); Group D: furan derivatives (originating from hemicellulose) (furans, furanons, furfurals); Group E: various oxygenated aromatic compounds that were not identified as phenolics (benzaldehyde/acetophenone, naphthalenols, biphenylols), Group F: lignin-derived phenolics (phenols, catechols, anisols, guaiacols, syringols); and unknown oxygenates. These unknown oxygenates were matched only with compounds that contained oxygen but had relatively low match quality to the NIST MS database.

One of the uncertainties inherent with gas chromatographic analysis of biocrudes is the actual percentage of the initial sample that is detected. Comparing the maximum oven temperatures in the GCxGC instruments used in this study (300°C and 225°C, respectively) to the simulated distillation results suggests that, at a minimum, 50-75% of biocrude F1 should be detectable and 25-55% of biocrudes F3 and F4 should

be detectable. However, some components, like levoglucosan, have higher boiling points compared to the sample oven temperatures but are abundant peaks in the chromatograms, so these percentages can be considered lower limits. In a previous study[23], the most abundant compounds identified in the chromatogram were quantified revealing that 22-47% of total sample volume was accounted for in the biocrude samples. Comprehensive, quantified GC/MS sample analysis is quite difficult but, within these limitations, the relative differences can be very informative.

Table 4: Physical properties and chemical composition of the non-fractionated CFP biocrudes (wet basis)

CFP biocrude	Feed F1	Feed F3	Feed F4	Feed F5
S, wt ppm (D4294)	27.0	108.1	101.8	58.2
N, wt ppm (D5762)	708.2	986.7	966.9	-
H, wt% (D7171)	8.3	7.28	7.02	6.49
O, wt% (elemental)	17	25.5	28	28.8
C, wt% (D5291)	73.9	64.5	62.9	62.6
Moisture content (wt%)	8.00	9.35	9.85	10.38
Total Inorganic (wt ppm)	33.7	40.0	40.5	184.9
Ca, wt ppm	18.4	15.5	18.8	95.0
Fe, wt ppm	5.8	4.0	3.0	12.6
K, wt ppm	1.5	2.5	3.2	13.3
Mg, wt ppm	1.3	3.1	3.3	21.1
Na, wt ppm	4.3	10.7	10.4	39.4
P, wt ppm	1.7	1.1	1.6	3.5
Si, wt ppm	0.7	3.1	0.2	< 0.1
Simulated Distillation (D7213)				
0.5 wt% (IBP), °C	-	85	86	-
5 wt%, °C	123	143	147	-
10 wt%, °C	143	173	175	-
20 wt%, °C	171	208	209	-
30 wt%, °C	188	234	238	-
40 wt%, °C	203	258	262	-
50 wt%, °C	220	288	292	-
60 wt%, °C	242	331	335	-
70 wt%,°C	272	360	361	-
80 wt%, °C	328	394	397	-
90 wt%, °C	394	445	450	-
95 wt%. °C	450	486	492	-
99.5 wt% (FBP), °C	554	558	564	-

The GC×GC-FID results for the non-fractionated biocrudes and WIS fractions of the biocrudes dissolved in THF are presented in Figure 2 and Figure 3, respectively. The data used to generate these plots is provided in the Supplemental Information (Table S1 and Table S2, respectively). The GC×GC-FID data of the non-fractionated biocrudes showed that the least oxygenated biocrude F1 contained the highest relative concentration of aliphatics, aromatics and aliphatic ketones and aldehydes. On the other hand, biocrudes F4 and F5 had higher concentration of oxygenated aromatics and phenolic compounds belonging to Groups E and F, respectively. Specifically, the analysis revealed that F5 had the highest amount of Group F compounds (catechols and alkylphenols). It is also worth pointing out that anisols (methoxybenzenes) were present in higher concentrations in F1 than in the other biocrudes. Additionally, F1 had the least amount of Group E compounds (hydroxylated aromatics such as naphthalenols, biphenylenols, and phenathrenols). Overall, the relative amount of furan derivatives such as furanones, hydroxyfurans, and furfuryl alcohols were low in all the biocrudes.

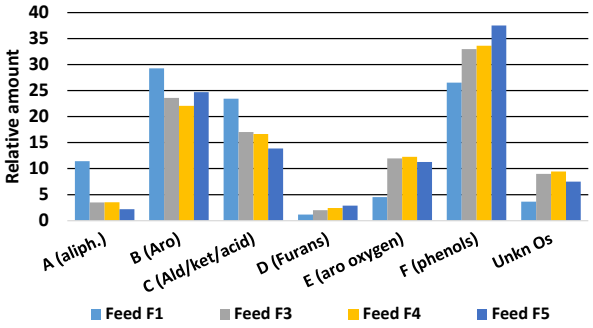

Figure 2: Bar plot showing the relative amounts (area %) as determined by GC×GC-FID (average of duplicate analyses) of integrated compound classes in the non-fractionated CFP biocrudes.

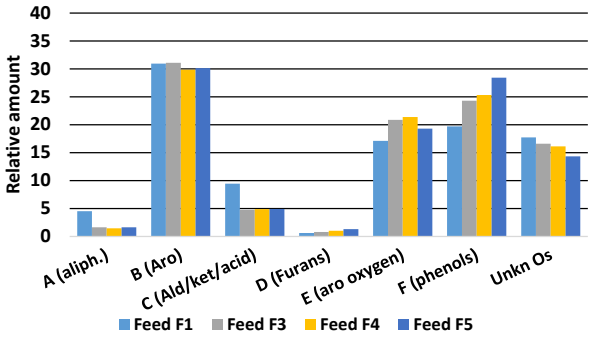

Figure 3: Bar plot showing the relative amounts (area %) as determined by GC×GC-FID (average of duplicate analyses) of integrated compound classes in the water-insoluble THF fractions of CFP biocrudes.

Compared to the WIS fractions, the non-fractionated biocrudes were found to contain higher relative concentrations of aliphatics (+26 to +60%), less aromatics (-6 to -35%), more aliphatic acids, aldehydes and ketones (+60 to +72%), more furan derivatives (+48 to +61%), less various oxygenated non-phenolics aromatic compounds (-71 to -277%), and more phenolics (+24 to +26%). Overall, the non-fractionated biocrudes contain more oxygenated compounds than the WIS THF fractions, as expected. Figure 4 shows that the relative amount of aliphatics correlates well with the hydrogen content while the amount of phenolics also correlates well with the oxygen content (R^2 values of 0.91 and 0.87, respectively). These trends justify the quantification method used for the GC×GC-FID data.

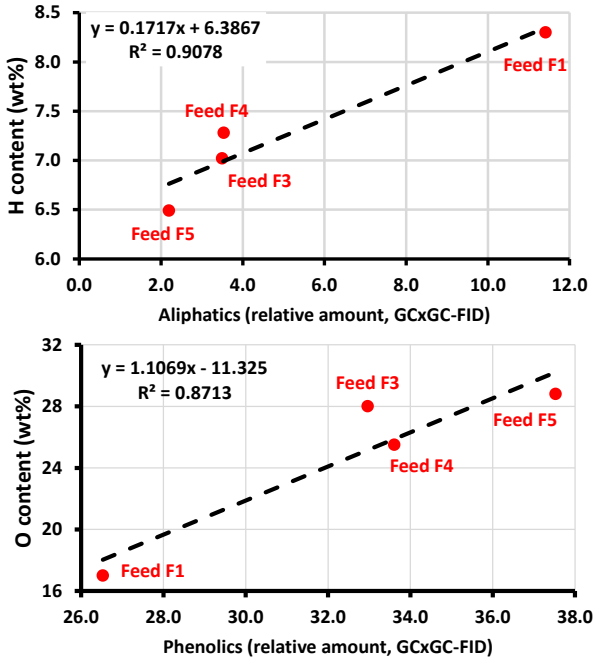

Figure 4: Correlations observed between; hydrogen content and aliphatics, and O content and phenolics, in CFP biocrudes.

Further analysis of the biocrudes was performed by ^{13}C-NMR spectroscopy since it is difficult to completely analyze the composition by GC. Table 7 shows a summary of the relative percent carbon content of eight carbon types present in the feeds. The ^{13}C-NMR spectra for the biocrudes are provided in the Supplemental Information (Figure S1, Figure S2, Figure S3, and Figure S4). The eight main functional group carbon types are based on the signals within the following chemical shifts (δ, ppm): aliphatic hydrocarbons (δ 0-45 ppm); methoxy carbon (-OCH3) in phenolics (δ 45-57 ppm); levoglucosan, anhydrosugars, alcohols, ethers (57-105 ppm); aromatic C–H bonds (δ 105-125); aromatic C–C bonds (δ 125-140); aromatic C–OH bond (δ 140-160); C=O in carboxylic acids and derivatives (δ 160 -180 ppm); and C=O in aldehydes and ketones (δ 180 -220 ppm). The signals from these chemical shifts were integrated and their relative percent carbon content for each category are reported for each biocrude. In general, the ^{13}C-NMR data supports the GC data. F1 contained the highest concentration of aromatic hydrocarbons and aliphatic ketones/aldehydes as shown by the relative carbon content of aromatic C–C bonds (δ 125-140) and C=O groups (δ 180 -220 ppm) respectively. Biocrudes F4 and F5 had the highest concentration of aromatic C–OH carbon indicating the presences of phenolic compounds as was shown by the GC×GC-FID data. Of note, the high carbon content of the methoxy carbon (-OCH3) in F3 and F4 suggest that those biocrudes had relatively higher concentration of methoxylated phenolics. It is worth pointing out that the ^{13}C-NMR data showed that the biocrude F5 had the highest concentration of oxygenated species such as levoglucosan, anhydrosugars, alcohols, ethers with carbon signals within 57-105 ppm.

Table 5: ^{13}C-NMR of the non-fractionated CFP biocrudes (Relative Percentage carbon total)

Carbon Type	Chemical Shift, δ (ppm)	Percentage carbon			
		FEED F1	FEED F3	FEED F4	FEED F5
Aliphatic hydrocarbons	0-45	31.8	32.8	38.5	23.0
Methoxy (-OCH3) in phenolics	45-57	3.3	4.1	4.3	2.0
Anhydrosugars, alcohols, ethers	60-105	0.5	4.1	4.3	18.4
Aromatic C–H bonds	105-125	27.0	27.1	22.1	24.0
Aromatic C–C bonds	125-140	25.6	19.8	16.0	17.4
Aromatic C–OH bond	140-160	7.9	8.9	11.9	12.1
C=O groups (carboxylic acids and derivatives)	160-180	2.0	2.0	1.9	2.2
C=O groups (aldehydes and ketones)	180-220	1.9	1.2	1.0	1.0

Based on the physical and chemical characterization of the four biocrudes, a hypothesis regarding how well these four CFP biocrudes will upgrade can be tested. Based on the total amount of metal contaminants in the biocrude, F5 would be expected to be the most difficult to upgrade followed by F4 and F3. F1 has the least metal contaminants suggesting that it would be easiest to upgrade. A similar expectation for relative upgrading performance would also be expected based on the oxygen content and hydrogen content of the CFP biocrudes. The simulated distillation curves also suggest that F1 contains the higher fraction of lower boiling range components and should thus be the easiest to upgrade.

Trends observed during the hydrotreating tests

Table 6 shows a summary of average product yields from the hydrotreating of biocrude feeds F1, F3, and F4. Of note, hydrotreating of Feed F5 did not last long enough to reach steady state so a reliable material balance could not be performed. The mass balances were above 95 wt% and the carbon balances were between 89% and 97%. On average, F3 resulted in the highest HDT product oil yield (77.8 wt%) and the lowest aqueous fraction (13.18 wt%), and product gas (5.53). All three feeds had high carbon efficiencies; 83-88% of the initial biocrude carbon was recovered in the HDT product oil. It is worth pointing out that Feed F1 resulted in a relatively high carbon loss to the product gas probably due to the high concentration of short-chain ketones and aldehydes as shown by the GCxGC and ^{13}C-NMR analyses. Nevertheless, F1 consumed the least amount of hydrogen (0.04677 g of H_2/g of dry bio-oil) which is a result of its low oxygen content (17 wt%). More details on the hydrotreating results from Feed F3 and F4 have been reported elsewhere in the literature.[40] Overall, the HDT product oil yields from the CFP biocrudes F1, F3, and F4 are comparable or even higher than previous work published in the literature.[28, 45-48]

Table 6: Summary of average product yields from the hydrotreating tests

HDT experiment	Exp. A	Exp. B	Exp. C
Biocrude Feed	Feed F4	Feed F3	Feed F1
Mass yield of product oil, wt%	73.08	77.80	71.90
Mass yield of aqueous fraction, wt%	16.90	13.18	16.00
Mass yield of product gas yield, wt%	6.12	5.53	7.33
Mass balance, wt%	96.10	96.50	95.22
Carbon yield of product oil, %	83.42	89.05	87.65
Carbon yield of aqueous fraction, %	0.41	0.22	0.25
Carbon yield of product gas, %	5.32	5.05	8.41
Carbon balance, %	89.18	94.33	96.30
H_2 consumed, g of H_2/g of dry bio-oil	0.06652	0.07075	0.04677

Changes in selected physical properties and chemical composition of the upgraded products as a function of time on stream from the CFP biocrude hydrotreating pilot tests are shown in Figure 5. The details of the physicochemical characteristics of the hydrotreated products from each experiment are provided in the Supplemental Information (Table S3, Table S4, Table S5, and Table S6). HDO catalyst deactivation is evident in all hydrotreating experiments since the oxygen content, nitrogen content, and specific gravity of the samples increases as a function of time on stream while the hydrogen content decreases. However, the rate of HDO catalyst deactivation, estimated as the rate of change in hydrogen, oxygen, and nitrogen contents and specific gravity, is different for each CFP biocrude. Suspected catalyst deactivation mechanisms include coke formation, pore blocking by contaminants, and catalyst desulfiding, but other unidentified causes may also be occurring. Coke formation is expected to be the dominant deactivation mechanism during these relatively short duration experiments (365 maximum run hours), while poisoning by trace impurities (like phosphorous, alkali metals, and other ash components) and desulfiding would only be evident during much longer (1000+ hours) upgrading experiments. In extreme cases coke formation can lead to reactor plugging in concert with the condensation of phenols and carbonyl compounds that can form polymers, for example.[49, 50] Numerous studies have targeted carbonyl removal with mild hydrotreating for bio-oil stabilization[50], yet the characterization of the whole biocrude feeds (^{13}C NMR in Table 5 and the GCxGC-FID results presented in Figure 2) indicate that the carbonyl content of the biocrude feeds is quite similar. In fact, Feed F1 actually has the highest carbonyl content but was the easiest to hydrotreat. The ^{13}C-NMR results in Table 5 do highlight that Feed F5 has the highest levoglucosan content. A recent study on catalytic hydrotreating of the pyrolytic sugar and pyrolytic lignin fractions of bio-oil suggests that thermal polymerization of levoglucosan and other anhydrosugars form higher molecular weight species that lead to coke deposits on the hydrotreating catalyst.[51] Thermal polymerization was not evident during pyrolytic lignin hydrotreating. Therefore, even though the hydrotreating experiments reported on in the literature were conducted in a batch reactor, their results are consistent with the rapid plugging experienced during biocrude F5 upgrading. It is also worh pointing out that the heavy end of the simulated distillation boiling curve measured for the upgraded samples increases with increasing run hours. In fact, the T95 of the upgraded products actually exceeds the T95 of all the biocrudes except F1. An enhanced heavy end formation has also been observed during vegetable oil hydrotreating. Cyclization and dehydrogenation reactions are thought to cause the heavy end and aromatic formation.[52, 53] A similar mechanism could also apply to upgrading biocrudes with relatively high phenolic contents.

The results presented in the graphs shown in Figure 5 suggest the following trends for HDO catalyst deactivation during CFP biocrude hydrotreating. The deactivation rate appears to be the lowest during biocrude F1 upgrading. This feed contains the most aliphatic hydrocarbons and the lowest oxygen content and also has the lowest simulated distillation end boiling point of the four biocrudes studied. The change in operating conditions (weighted average bed temperature is 10°C lower and H_2/oil ratio is 10% higher) for upgrading biocrude F3 and F4, respectively have minimal but measurable impact on the deactivation rates. The highest HDO catalyst deactivation rate is observed for biocrude F5. This feed has the highest oxygen content, contains the most contaminants and phenolics, and has the lowest concentration of hydrocarbons.

There is no consensus that deactivation rates obtained in pilot-scale units can be extrapolated to commercial catalyst performance. The design and operation of specific units can influence catalyst performance; however, if similar tests are run in the same unit, at similar conditions and with the same catalyst, the relative catalyst deactivation rates may provide some qualitative insights into catalyst performance. The simplest way to compare deactivation rates is to assume a linear correlation with respect to run hours. An example is given in Figure 6, where the changes in O content of the products are plotted with respect to run hours.

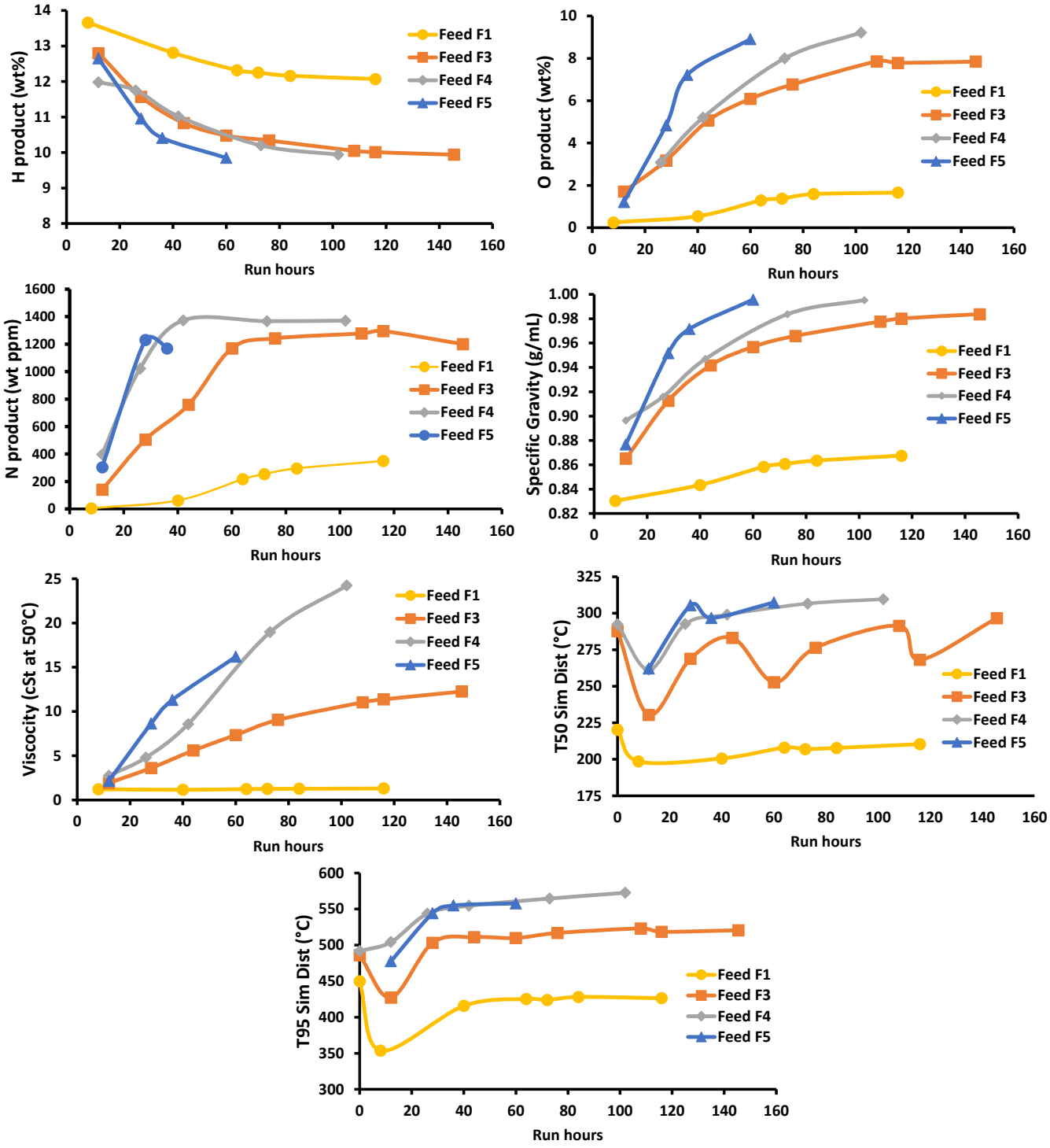

Figure 5: Variation of selected physical properties and changes in chemical composition of the HDO products collected as a function of run hour during the various HDT tests.

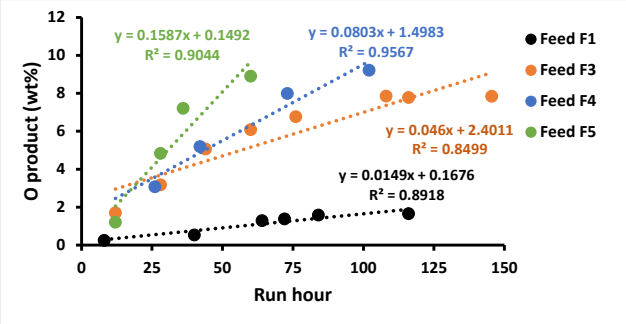

Figure 6: Oxygen content in upgraded products from HDT of CFP biocrudes with respect to run hours. Dotted lines represent a linear fit through the data. The slope, intercept, and correlation coefficient are provided for each fit.

Table 7 compares the initial biocrude composition with the trends observed with respect to the changes in upgraded product composition during the CFP biocrude hydrotreating. The role of the solid acid catalyst in the CFP process is to deoxygenate biomass pyrolysis vapors to produce a more thermally stable biocrude. The concentration of aliphatic acids and anhydrosugars in our CFP biocrude tends to be much lower compared to other bio-oils from non-catalytic biomass pyrolysis. The HDO chemistry discussed by Gollakota et al.[26] explains that ketones are easily hydrogenated above 200°C and carboxylic acids can be hydrogenated under HDO conditions. However, the CFP biocrude is highly aromatic and still contains oxygenated components, both phenolics and non-aromatic oxygenates.

In a recent review,[31] Furimsky describes the complex reactions that occur during biocrude hydroprocessing that are consistent with the results present in this study. For example, sequential HDO of methoxyphenols produces phenol. However, it is known that hydrogenation of the aromatic ring to produce cyclohexanol is the preferred pathway compared to phenol HDO to produce benzene.

The biocrude feeds upgraded in this study are highly aromatic and contain a high concentration of methoxyphenols. During the initial stages of biocrude upgrading, when the hydrotreating catalyst activity is high, HDO converts the oxygenates to aliphatic hydrocarbons, naphthenes, and aromatic hydrocarbons in the upgraded products. The non-phenolic oxygenates and some of the phenolics are deoxygenated.

Hydrogenation of some of the aromatics originally in the biocrude feed seems to occur at the highest hydrotreating catalyst activity; however, ring saturation decreases as the hydrotreating catalyst deactivates over time, suggested by the increased aromatic content in the upgraded products. This is evident in Table 7 when the initial biocrude feed compositions are compared to the initial upgraded product compositions. Feed F1 contains 4.5% aliphatic hydrocarbons yet the initial upgraded products contain 89% aliphatic hydrocarbons while the initial aromatic content is only 8% suggesting saturation of the aromatic intermediates produced during HDO. For Feeds F3, F4, and F4, the aromatic content in the initial upgraded products equals or exceeds the aliphatic hydrocarbon content.

The HDO activity also decreases as suggested by the increased phenolic content of the upgraded products. The aliphatic content of the upgraded products at the end of the experiments decreases significantly as the phenolic content increases. Yet the HDO activity is high enough to convert non-phenolic oxygenates to hydrocarbons. While the concentration of aromatics, aliphatics and phenolics increase with upgrading time on stream it appears that there are higher concentrations in the final upgraded products compared to the biocrude feeds. This also suggests that multifunctional oxygenated aromatics and hydrocarbons are still partially deoxygenated even after the HDO catalyst has deactivated.

Table 7: Trends observed with respect to changes in composition of WIS fractions of the upgraded products during HDT pilot plant tests compared to the starting biocrude feed

GCxGC-FID of WIS Fraction (%-area)		Feed	Upgraded Products	
			Start of run	End of run
Group A (aliphatics)	F1	4.5%	89%	29%
	F3	1.6%	45%	8%
	F4	1.5%	23%	9%
	F5	1.6%	45%	6%
Group B (aromatics)	F1	31%	8%	31%
	F3	31%	43%	50%
	F4	30%	64%	51%
	F5	30%	47%	49%
Group C (acids, ketones, aldehydes)	F1	9%	0.4%	0.2%
	F3	5%	0.5%	0.3%
	F4	5%	0.3%	1%
	F5	5%	0.4%	0.6%
Group D (furan derivatives)	F1	0.6%	---	---
	F3	0.8%	---	---
	F4	17%	---	---
	F5	1.3%	---	---
Group E (non-phenolic oxygenates)	F1	17%	2%	2%
	F3	21%	3%	9%
	F4	21%	2%	9%
	F5	19%	1.5%	11%
Group F (phenolics)	F1	20%	---	---
	F3	24%	7%	32%
	F4	25%	11%	30%
	F5	28%	6%	33%

Conclusions

Four biocrudes produced from loblolly pine in a 1TPD catalytic biomass pyrolysis unit were hydrotreated in a pilot-scale hydroprocessing unit with two downflow fixed bed redactors. The deactivation rate of the HDO catalyst activity was evaluated based on the physical properties and chemical composition (determined by GC×GC-MS and GC×GC-FID) of the upgraded products as a function of time on stream. It was possible to correlate the relative deactivation rates with the initial CFP biocrude physical properties and chemical composition. Of the four CFP biocrude evaluated in this study, it appears that the higher the oxygen content the higher the HDO catalyst deactivation rate. Another key result was that, in three out of four experiments, hydrotreated products have a higher end boiling point than the starting biocrude. During the hydrotreating tests, aliphatic acids, ketones, aldehydes, furan derivatives were fully removed while aromatics, aliphatics and

phenolics increased and exceed those of the biocrude at the end of the run. Overall, the use of less oxygenated biocrude causes less hydrotreating catalyst deactivation during upgrading.

Author Contributions

S. Verdier: conceptualization, formal analysis, validation, project administration, writing – original draft. O. Mante: conceptualization, formal analysis, validation, resources, writing – original draft, writing – review & editing. A. Hansen: formal analysis, investigation, validation, writing – review & editing. K. Poulsen: formal analysis, investigation, validation. J. Christensen: formal analysis, data curation, investigation, methodology, supervision, validation, writing – original draft, writing – review & editing. N. Ammtizboll: investigation, formal analysis. J. Gabrielsen: conceptualization, data curation, validation. D. Dayton: conceptualization, funding acquisition, methodology, project administration, validation, visualization, writing – original draft, writing – review & editing.

Conflicts of interest

There are no conflicts to declare.

Acknowledgements

D.C. Dayton and O.D. Mante (RTI International) would like to acknowledge financial support from the U.S. Department of Energy, Office of Energy Efficiency and Renewable Energy, Bioenergy Technologies Office under contract EE-0005358 (Catalytic Upgrading of Thermochemical Intermediates to Hydrocarbons). The authors would also like to acknowledge Jonathan Peters, David Barbee and Michael Carpenter for supporting the CFP pilot-scale experiment, as well as Kelly Amato for providing analytical support.

References

1. *World Energy Outlook 2018*, International Energy Agency, 2018.
2. R. Estevez, L. Aguado-Deblas, F. M. Bautista, D. Luna, C. Luna, J. Calero, A. Posadillo and A. A. Romero, *Catalysts*, 2019, **9**, 1033.
3. M. Ameen, M. T. Azizan, S. Yusup, A. Ramli and M. Yasir, *Renewable and Sustainable Energy Reviews*, 2017, **80**, 1072-1088.
4. L. Brennan and P. Owende, *Renewable and Sustainable Energy Reviews*, 2010, **14**, 557-577.
5. T. Dickerson and J. Soria, *Energies*, 2013, **6**, 514-538.
6. S. N. Naik, V. V. Goud, P. K. Rout and A. K. Dalai, *Renewable and Sustainable Energy Reviews*, 2010, **14**, 578-597.
7. P. S. Nigam and A. Singh, *Progress in Energy and Combustion Science*, 2011, **37**, 52-68.
8. A. V. Bridgwater, *Biomass and Bioenergy*, 2012, **38**, 68-94.
9. S. Hansen, A. Mirkouei and L. A. Diaz, *Renewable and Sustainable Energy Reviews*, 2020, **118**, 109548.
10. A. P. P. Pires, J. Arauzo, I. Fonts, M. E. Domine, A. F. Arroyo, M. E. Garcia-Perez, J. Montoya, F. Chejne, P. Pfromm and M. Garcia-Perez, *Energy & Fuels*, 2019, **33**, 4683-4720.
11. S. Mannonen, *Journal*, 2014, 47-48.
12. M. C. Vásquez, E. E. Silva and E. F. Castillo, *Biomass and Bioenergy*, 2017, **105**, 197-206.
13. R. Secretariat, *Renewables 2018 Global Status*, REN21 - Renewable Energy Policy Network for the 21st Century, Paris, 2018.
14. D. López Barreiro, B. R. Gómez, F. Ronsse, U. Hornung, A. Kruse and W. Prins, *Fuel Processing Technology*, 2016, **148**, 117-127.
15. S. M. Al-Salem, A. Antelava, A. Constantinou, G. Manos and A. Dutta, *Journal of Environmental Management*, 2017, **197**, 177-198.
16. R. Miandad, M. A. Barakat, A. S. Aburiazaiza, M. Rehan and A. S. Nizami, *Process Safety and Environmental Protection*, 2016, **102**, 822-838.
17. S. D. Anuar Sharuddin, F. Abnisa, W. M. A. Wan Daud and M. K. Aroua, *Energy Conversion and Management*, 2016, **115**, 308-326.
18. A. Rowhani and T. Rainey, *Energies*, 2016, **9**, 888.
19. J. D. Martínez, N. Puy, R. Murillo, T. García, M. V. Navarro and A. M. Mastral, *Renewable and Sustainable Energy Reviews*, 2013, **23**, 179-213.
20. D. Mohan, C. U. Pittman and P. H. Steele, *Energy & Fuels*, 2006, **20**, 848-889.
21. R. H. Venderbosch, *ChemSusChem*, 2015, **8**, 1306-1316.
22. D. C. Dayton, J. R. Carpenter, A. Kataria, J. E. Peters, D. Barbee, O. D. Mante and R. Gupta, *Green Chemistry*, 2015, **17**, 4680-4689.
23. O. D. Mante, D. C. Dayton, J. R. Carpenter, K. Wang and J. E. Peters, *Fuel*, 2018, **214**, 569-579.
24. T. M. H. Dabros, M. Z. Stummann, M. Høj, P. A. Jensen, J.-D. Grunwaldt, J. Gabrielsen, P. M. Mortensen and A. D. Jensen, *Progress in Energy and Combustion Science*, 2018, **68**, 268-309.
25. P. M. Mortensen, J. D. Grunwaldt, P. A. Jensen, K. G. Knudsen and A. D. Jensen, *Applied Catalysis A: General*, 2011, **407**, 1-19.
26. A. R. K. Gollakota, M. Reddy, M. D. Subramanyam and N. Kishore, *Renewable and Sustainable Energy Reviews*, 2016, **58**, 1543-1568.
27. D. C. Elliott, *Energy & Fuels*, 2007, **21**, 1792-1815.
28. A. H. Zacher, M. V. Olarte, D. M. Santosa, D. C. Elliott and S. B. Jones, *Green Chemistry*, 2014, **16**, 491-515.
29. M. Al-Sabawi and J. W. Chen, *Energy & Fuels*, 2012, **26**, 5373-5399.
30. J. A. Melero, J. Iglesias and A. Garcia, *Energy & Environmental Science*, 2012, **5**, 7393-7420.
31. E. Furimsky, *Catalysis Today*, 2013, **217**, 13-56.
32. M. S. Talmadge, R. M. Baldwin, M. J. Biddy, R. L. McCormick, G. T. Beckham, G. A. Ferguson, S. Czernik, K.

A. Magrini-Bair, T. D. Foust, P. D. Metelski, C. Hetrick and M. R. Nimlos, *Green Chemistry*, 2014, **16**, 407-453.

33. D. C. Elliott, D. Meier, A. Oasmaa, B. Van De Beld, A. V. Bridgwater and M. Marklund, *Energy & Fuels*, 2017, **31**, 5111-5119.
34. J. R. Ferrell III, M. V. Olarte, E. D. Christensen, A. B. Padmaperuma, R. M. Connatser, F. Stankovikj, D. Meier and V. Paasikallio, *Biofuels, Bioproducts and Biorefining*, 2016, **10**, 496-507.
35. A. Oasmaa and D. Meier, *J. Anal. Appl. Pyrolysis*, 2005, **73**, 323-334.
36. M. Stas, J. Chudoba, D. Kubicka, J. Blazek and M. Pospisil, *Energy & Fuels*, 2017, **31**, 10283-10299.
37. M. Stas, D. Kubicka, J. Chudoba and M. Pospisil, *Energy & Fuels*, 2014, **28**, 385-402.
38. C. M. Michailof, K. G. Kalogiannis, T. Sfetsas, D. T. Patiaka and A. A. Lappas, *Wiley Interdiscip. Rev. Energy Environ.*, 2016, **5**, 614-639.
39. P. K. Kanaujia, Y. K. Sharma, M. O. Garg, D. Tripathi and R. Singh, *J. Anal. Appl. Pyrolysis*, 2014, **105**, 55-74.
40. O. D. Mante, D. C. Dayton, J. Gabrielsen, N. L. Ammitzboll, D. Barbee, S. Verdier and K. G. Wang, *Green Chemistry*, 2016, **18**, 6123-6135.
41. M. Kristensen, A. B. Hansen, O. D. Mante, D. C. Dayton, S. Verdier, P. Christensen and J. H. Christensen, *Energy & Fuels*, 2018, **32**, 5960-5968.
42. R. L. Ware, R. P. Rodgers, A. G. Marshall, O. D. Mante, D. C. Dayton, S. Verdier, J. Gabrielsen and S. M. Rowland, *Sustain. Energ. Fuels*, 2020, **4**, 2404-2410.
43. A. Oasmaa, E. Kuoppala and D. C. Elliott, *Energy & Fuels*, 2012, **26**, 2454-2460.
44. A. Oasmaa, E. Kuoppala and Y. Solantausta, *Energy & Fuels*, 2003, **17**, 433-443.
45. D. C. Elliott, H. Wang, R. French, S. Deutch and K. Iisa, *Energy & Fuels*, 2014, **28**, 5909-5917.
46. D. C. Elliott, H. Wang, M. Rover, L. Whitmer, R. Smith and R. Brown, *ACS Sustainable Chemistry & Engineering*, 2015, **3**, 892-902.
47. M. V. Olarte, A. H. Zacher, A. B. Padmaperuma, S. D. Burton, H. M. Job, T. L. Lemmon, M. S. Swita, L. J. Rotness, G. N. Neuenschwander, J. G. Frye and D. C. Elliott, *Topics in Catalysis*, 2016, **59**, 55-64.
48. N. Schwaiger, D. C. Elliott, J. Ritzberger, H. Wang, P. Pucher and M. Siebenhofer, *Green Chemistry*, 2015, **17**, 2487-2494.
49. E. Laurent, A. Centeno and B. Delmon, in *Catalyst Deactivation 1994*, 1994, vol. 88, pp. 573-578.
50. A. H. Zacher, D. C. Elliott, M. V. Olarte, H. Wang, S. B. Jones and P. A. Meyer, *Biomass and Bioenergy*, 2019, **125**, 151-168.
51. W. Yin, M. V. Alekseeva, R. H. Venderbosch, V. A. Yakovlev and H. J. Heeres, *Energies*, 2020, **13**, 285.
52. G. N. Darocha, D. Brodzki and G. Djegamariadassou, *Fuel*, 1993, **72**, 543-549.
53. I. Mihail and P. S. Zoran, in *Soybean - Applicaitons snd Technology*, ed. T. Z. Ng, InTech, 2011, DOI: 10.5772/621, ch. 21, p. 24.

Abbreviations

CFP	Catalytic Fast Pyrolysis
FCC	Fluid Catalytic Cracking
FID	Flame Ionization Detector
GC×GC	Comprehensive two-dimensional gas chromatography
HDO	Hydrodeoxygenation
LHSV	Liquid Hourly Space Velocity (Feed flow(l/h)/Catalyst volume (l))
MS	Mass Spectrometry
SG	Specific Gravity
THF	Tetrahydrofuran
WABT	Weighted Average Bed Temperature
WIS	Water Insoluble